AO13 Aerosol sampling

supervisor: Dr Daniel Peters
March 2008

Abstract

The vertical distribution of aerosol properties in the atmosphere, for example- salt crystals, sand, ablated soils, and aviation derived black carbon soot in the upper troposphere and lower stratosphere is very poorly quantified. Yet they have a significant impact on radiative transfer in an aerosol laden atmosphere. There has been relatively little research involving direct sampling of aerosol particles at altitude, and published studies have involved aircraft mounted samplers.

A cheap autonomous sonde mounted sampler was designed and constructed together with functional sonde sub-systems, to enable sampling to be conducted over the UK at altitudes up to 30km, with multiple samples taken in different altitude ranges. The sampling device was designed to enable examination with a scanning electron microscope to determine composition, morphology, and particle concentrations to be inferred.

1 Introduction

Aerosol research is a very active field, with particular bearing on many aspects of atmospheric physics. However, the majority of non ground based studies have involved inferring measurements from satellite, not direct measurements or sampling. Blake and Kato [1], and Pusechel at al [3], employed NASA ER-2 and DC-8 research aircraft mounted sampling devices. These aircraft have altitude ceilings of 21Km and 12km respectively, lower than sonde flights, which can reach 30km with ease. In Europe there is also the CARIBIC program [4], employing an Airbus A340 and Boeing 767 300ER in published research programs. Physical sampling for later laboratory analysis allows chemical composition to be determined, along with particle morphology [1].

Meanwhile, the falling price of electronic hardware including GPS receivers and communication equipment has sparked interest in the development of low-cost sounding units to supplement the traditional radiosonde network. A sonde based system is considerably cheaper and more flexible than the aforementioned systems, can sample a greater altitude range, and is not limited by air traffic control regulations to the same extent. This project was inspired by such novel alternative sounding methods, which have recently been pioneered in the UK by the UK high altitude society [11], and Cambridge university spaceflight [12].

Stratospheric sampling conditions: From Blake and Kato [1] number densities for black carbon soot particles are in the $10^5 m^{-3}$ range. These typically consist of a chain structure of globules of around 50nm diameter. The morphology of the particles, and their evolution over time are of particular interest, as is the role of aviation in their production. Sulphuric acid particles are also found.

Tropospheric sampling conditions: Tropospheric particles are more diverse, primary aerosols of ablated soil particles, sand, and sea salt aerosol are found. Secondary aerosols such as ammonium nitrate are directly formed from the gas phase. Number densities are over two or-

ders of magnitude higher than for stratospheric aerosol.

Aviation is thought to be the largest contributor to black carbon in the stratosphere[1]. During the past few decades, air traffic has increased at a high rate, (see UK aviation CO_2 forecasts 2005-2050 figure 1.3 [9]). This shows that since the study by Blake et al in 1995, UK CO_2 emissions have increased by 50%. This would imply a similar increase in black carbon emission, however, this may have been confounded to some degree by a cleaner aircraft fleet. This project aims to enable a direct measurement of the current level of black carbon in the Stratosphere and upper Troposphere.

2 Methods

2.1 Aims

A set of aims were drawn up as follows;

1. Demonstrate and design an aerosol sampling device capable of sampling aerosol from the troposphere to stratosphere.
2. Obtain samples of aviation aerosol soot (black carbon) emission.

2.1.1 Science Requirements

From a consideration of the science aims, the list of requirements were drawn up;

1. The collection efficiency as a function of particle size should be well quantified
2. The sampler should collect a statistically significant sample
3. There should be statistically insignificant sample contamination
4. Non-volatile particles should be captured and stored without changes to their chemistry
5. If multiple samples are taken (e.g. differing altitude ranges) then cross contamination should be insignificant or at least well quantified

2.2 Hardware design considerations

A typical sonde flight will ascend to reach an apogee altitude of 20 to 30Km above mean sea level around 2 hours after launch. The latex envelope then bursts, leaving the payload to descend by parachute. Ground air temperature in the UK is usually in the 10 to 20°C range, and tropopause temperatures are typically around −50°C, so the payload experienced large temperature changes. The lower temperature limit lies outside the standard industrial temperature range used for electronics, which extends to −40°C. During descent into the troposphere, condensation is a significant risk due to the sonde payload being below the dew-point. The typical solution to these difficulties, adopted by members of UKHAS and others is a 25 to 50mm thick airtight[1] enclosure fabricated from extruded polystyrene or expanded polypropylene. This serves to protect sensitive components on landing, as well as allowing the electronics to increase the internal temperature to acceptable levels.

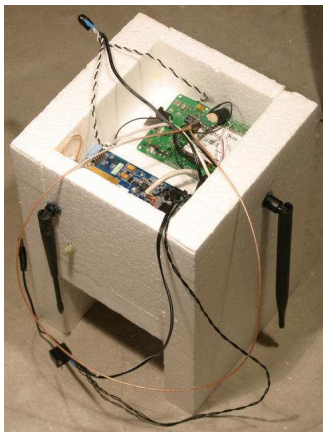

Figure 1: A typical sonde based on an embedded linux system

The avionics are critical to safely recovering the payload after landing, and again UKHAS[11] and CUSF[12] provide useful examples of how to design a successful system. Typically a central computer board based around a micro-controller, or an off the shelf single board Linux machine is used. The other electronic hardware is then interfaced with the central "motherboard", a minimal architecture consisting

[1] obviously an airtight closed cell foam enclosure would suffer structural failure due to internal overpressure during ascent, but assembly has been found to never be good enough to be completely airtight, although sufficient to prevent condensation

of GPS receiver, mobile phone/GSM module module, radio module, and a release mechanism to cut-down[2] Such a system typically requires in the order of 1 to 2 Watts of electrical power, and it has been found that lithium camera batteries, such as sold by energizer[13] offer the best performance, the data-sheet listing the absolute minimum operating temperature as -40°C.

The radio module is perhaps one of the more difficult components, in the UK OFCOM limits transmissions from high altitude balloons to 10mw on the 434MHz band, using a commercial transmitter module of a licenced design. It is possible to transmit radio-teletype at 300 baud on this band for several hundred kilometres by using a pulse shaping transmission scheme to modulate an FM transmitter. Members of the UK high altitude society have previously designed a system, but the source code has not been released, and there is no printed circuit board design for the project. With this in mind, in 2007 the author designed a radio module using an 8 bit AVR micro-controller, which was employed for the first time on this sonde.

A final consideration is mass, the civil aviation authority does not explicitly set mass limits on radiosondes, but bearing in mind health and safety, and insurance for the project, a mass limit of 2Kg was decided upon.

2.3 Instrument design process

The aerosol sampler designs considered were all drawn from Hinds [2], and evaluated on their suitability based on the science aims and hardware considerations, along with our budgetary limits of approximately £1000 for the entire system. From Blake and Kato[1], number densities of stratospheric particles are in the $10^4 m^{-3}$ to $10^5 m^{-3}$ range, so about 10^3 particles are required to provide statistically significant data for particle morphology and chemistry studies, if our instrument has a collection efficiency in the 10% range and we require 10^3 particles, a $1m^3$ air sample is required. If multiple samples are to be taken during the ascent, a reasonable sampling time might be around 40 minutes, or 2×10^3 seconds. This gives a flow rate of between 10^{-4} and $10^{-5} m^3 S^{-1}$ through the instrument.

In all the sampling techniques considered, particles are deposited onto some sampling surface for later analysis. For analysis of with a scanning electron microscope, a minimum number density on the sampling surface of 1 particle per $100\mu m^2$ seems reasonable[3]. For a sample of 10^2 to 10^3 particles, this corresponds to a sampling surface area 0.33mm^2 at most.

It is essential to ensure that the flow through the instrument is laminar to prevent aerosol deposition. Assuming that the airflow cross-section is larger than the sampling surface area (valid in all approaches accept 4), then with a cross section of 1mm^2 for our airstream through the instrument, an airspeed of at least 10ms^{-1} is required (at $10^{-5} m^3 s^{-1}$). The Reynolds number is given by

$$\frac{\rho v_s L}{\mu} = \frac{v_s L}{\nu} \tag{1}$$

For typical stratospheric flow, $\mu = 2.5 \times 10^{-5}$, and $\rho = 10^{-1} Kg/m^3$, so the Reynolds number is given by

$$\frac{10^{-1} v_s L}{2.5 \times 10^{-5}} = 4 \times 10^3 v_s L \tag{2}$$

Within circular pipes the critical Reynolds number is generally accepted to be 2300, where the Reynolds number is based on the pipe diameter and the mean velocity v_s within the pipe. Assuming the lower bound on volumetric sampling rate, i.e. 10^{-2}Litre s^{-1} then if our instrument consists of some circular pipe.

$$\pi L^2 V_s = 10^{-5} \tag{3}$$

so, if $Re < 2000$ then

$$V_s L < 0.5 \longrightarrow L \gtrsim 10^{-4} \tag{4}$$

in the lower troposphere, the Reynolds number will be an order of magnitude higher, so the condition on L will increase by an order of magnitude, but 1mm diameter is achievable, and lower

[2] "cut-down" is a radiosonde term meaning to trigger an early descent by releasing the balloon from the payload, for example to avoid landing in water

[3] simply by considering the difficulties inherent in using a scanning electron microscope to examine a sparsely populated sampling surface

flow rates will be required due to the higher volumetric number densities of particulates in the troposphere.

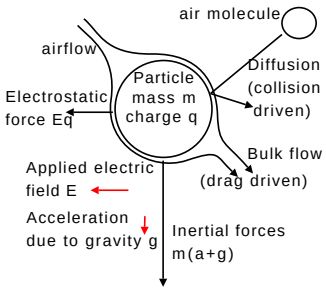

Figure 2: A look at the different effects influencing particle motion in the μm regime

So, in conclusion, achieving laminar flow is possible, but achieving a well characterised sampling efficiency, and a high particle density on the sampling surface is non trivial. Laminar flow is especially important for the first three methods, as existing studies have been in the laminar flow region, and collection efficiencies in the case of electrostatic and thermal precipitators especially drops off as we enter the turbulent flow regime. Four approaches were considered:

1. Thermal precipitator: as this system relies on a temperature gradient, it would require a heater, probably a resistance wire. Power limitations make this hard to achieve. As with a filter, achieving a high particle density per unit area of the deposition surface is difficult. A small heated area separated from the deposition target by an air gap would require a high airflow velocity between the two plates, limiting the collection efficiency. If the airflow becomes non laminar, collection efficiency will drop off greatly, and an accurate efficiency calculation would require careful calibration.

2. Impactor: This design has been used with success before by NASA on ER-2 and DC8 aircraft [5], however an aircraft mounted implementation can easily have a very high velocity airstream, and high volumetric flow rate, something that is harder to achieve on a sonde with power, weight and size limitations. A small scale impactor may work well for small ranges of particle size, but designing for a large range of particle sizes from the hundreds of nanometre diameter to several micron range is hard, due to the widely differing Reynolds numbers that the particles would experience. Despite research into existing designs, an existing design that was well studied and easily adapted for sonde use was not found.

3. Electrostatic precipitator: the operating principle uses a corona discharge to charge particles, and then an electric field to draw them out of the airflow onto a collection target. The most common design is so called single stage, employing a sharpened electrode opposite a deposition target, hence achieving both ionisation from the corona discharge, and deposition from the E field in a single step. Yung-Sung Cheng et al [6], Laskin and Cowin [7] and Aerosol technology[2] all describe similar designs, which are well suited to sonde use. Yung et al also found efficiency curves for their single stage precipitator, based on Morrow et al [8]. This technique has the advantage that a standard scanning electron microscope or SEM sample holder can be used as a target plane, simplifying the particle analysis considerably.

4. Filter: This would appear a natural choice, but with the low particle densities in the stratosphere, a high flow rate per area of filter is required. However, in the limiting case where our pump generates a vacuum, the pressure across the filter is limited to atmospheric pressure. At the low atmospheric pressure at such altitudes, it is thus impossible to reach the required differential pressure to achieve a usable particle density per unit area of filter with a pump downstream of the filter (flow through a filter is linear with differential pressure 6). A pump mounted upstream would lead to contamination and particle size bias problems. Also, the retrieval process would be extremely difficult with a fibre based filter- membrane filters would be similar to the other three techniques with regard to retrieval, but at the

Figure 3: The electrostatic precipitator was machined from perspex, with a piston at the inlet to prevent contamination

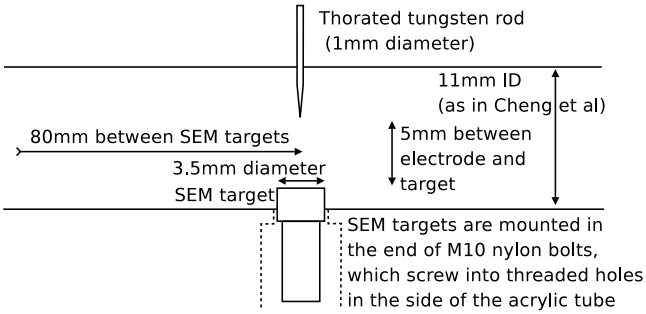

Figure 4: The design was based on Cheng et al, figure 1

expense of lower flow rate than fibre based filter.

The electrostatic precipitator was chosen as the sampling system, primarily due to the existing and well researched designs, and suitability for use in a small, lightweight and low power instrument.

The relatively high collection efficiency found by Yung et al suggests that an inline sampling system with multiple target/ioniser pin pairs would be effective. A three sample device was designed, based on three variants of the design from Morrow et al. mounted in series in a solid perspex tube. The use of multiple targets is an untried innovation.

Unfortunately this design cannot reach the

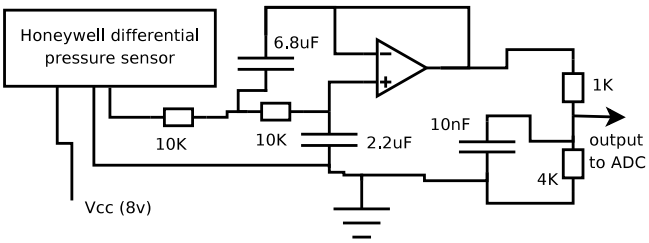

Figure 5: Circuit diagram of the Sallen-Key filter used for the differential pressure sensor

0.33mm^2 deposition area target calculated earlier, instead the deposition takes place over an area of around 6mm^2, around 20 times lower particle density. However, with good handling to avoid contamination, it should be possible to locate the particles with some microscope panning.

2.4 Avionics

For maximum flexibility the avionics system was designed around the atmel ngw100 embedded linux board. This enabled flight software to be easily tested on a PC running the ubuntu distro. Serial ports were then used to interface with a daughter-board, phone, radio module, and gps module. The cut-down directly connected to GPIO for improved reliability. The ngw100 pulses GPIO high then low on bootup, so a binary coded decimal decoder IC was used to drive the cut-down MOSFETs.

The daughter-board was designed around an atmel atmega168 8 bit micro-controller[4], mainly serving as an IO expander and ADC, but with the pulse width modulation output used to drive the pump on the sampling instrument. This arrangement allows for real time pump control based on an ADC reading from a differential pressure sensor connected across the filter between the precipitator tube and pump, as differential pressure is proportional to the flow rate (see equation 6).

However, equation 6 only holds for constant viscosity. Air viscosity is a function of temperature, as described by Sutherland's' equation

$$\eta = \eta_0 \frac{T_0 + C}{T + C} \left(\frac{T}{T_0} \right)^{3/2} \tag{5}$$

[4]also referred to as a μC

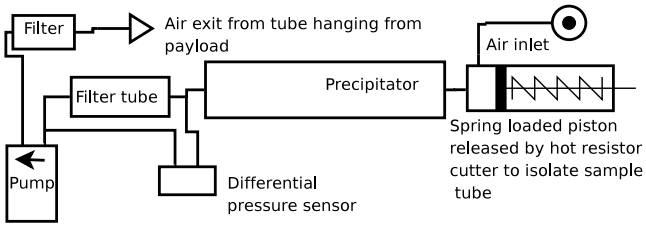

Figure 6: Flow diagram of the air sampling system

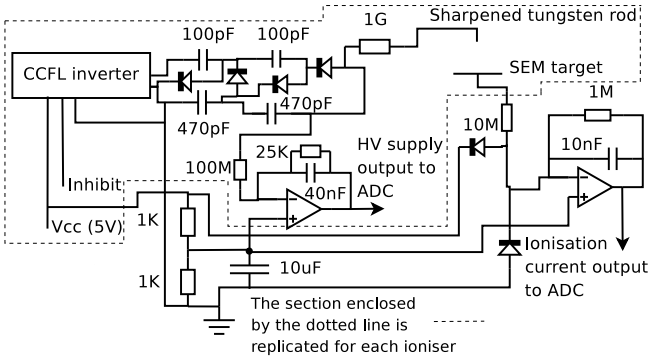

Figure 7: Circuit diagram of the electrostatic precipitator electronics

where C is Sutherland's constant (120K for air), T_0 is the reference temperature in kelvin (291.15K for air), and η_0 is the reference viscosity (1.827×10^{-5} for air).

Over the typical temperature range that the sonde might experience, this leads to a significant change in viscosity, such that using predicted temperatures for the current altitude wouldn't not give a sufficiently accurate result. Hence a semiconductor band-gap based sensor IC (LM94022) was placed inside the exit tube from the precipitator directly in the airflow. Unfortunately this was damaged by an mistake during testing, and was replaced by a thermistor and preamp circuit.

The precipitator itself requires a high voltage supply for operation. Research into commercial systems lead to the design of a simple low cost supply employing a cold cathode inverter, designed for LCD back-lights, and giving an output of approximately 700v ac, followed by a Cockroft Walton multiplier chain to boost the voltage (see Figure 7). Switching voltages in the

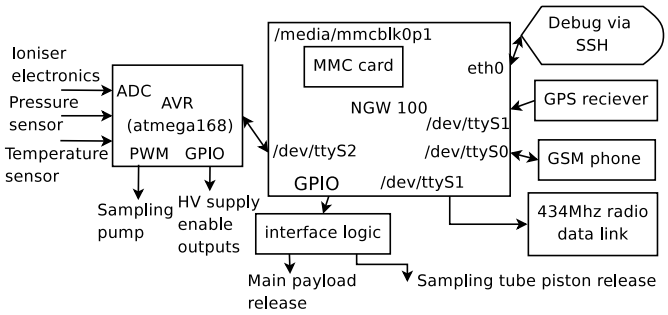

Figure 8: An overview of the payload as it appears from the software's perspective

Kv range using transistors is quite difficult, so three separate supplies were constructed, one for each sampling electrode. Due to the lower dielectric strength of air at low pressures, the two upper atmospheric supplies only had one multiplier stage, giving approximately 2.5Kv output, whereas the first stage supply had an output of approximately 5Kv. As suggested by Laskin and Cowin, 1GΩ resistors were placed between the HV supplies and the precipitator to stabilise the ionisation current. This had the additional advantage of ensuring high voltage safety, as the current is limited to a low level.

2.5 Software

There were two main pieces of software to be written, the main control code for the ngw100, in python, and the low level interface code for the μC, in c, and compiled with avr-gcc.

The default kernel on the ngw100 does not allow access to the three available serial ports, so a kernel recompile was needed. The pyserial module was then used to interface with the the ports. There is little free space on the ngw100 flash memory, so an 128MB MMC card was used to store data logs and mount python. As the 434MHz radio has a relatively high bit error rate, a reed-Solomon python module, written previously by the Author, was used to add forward error correction to the end of the data-packets, but leave the actual data human readable, to simplify ground station operation. The landing spot prediction code posted on the UK high alti-

tude society website [5] was ported to python, and the parachute drag constants rescaled to the 1.4 meter chute used for payload recovery. This was then combined with a polygon of the East Anglia coastline, and an "exclusion zone" north of London and east of Birmingham, to trigger the cutdown and avoid an urban or sea landing if necessary, and more basic routines for logging data and relaying telemetry. Communication with the phone was via the extended Hayes AT command set, and the GPS via the standard NMEA serial protocol.

The μC code made heavy use of procyon avrlib [10], a library simplifying tasks such as buffered serial IO and pulse width modulation.

Both programs are in the appendix, together with the radio modem source and the reed-Solomon module.

2.6 Experimental Testing

2.6.1 Aerosol flow testing

This was necessary to investigate precipitator performance, obtain collection efficiency data, and quantify the cross contamination between different electrode/SEM target pairs. An ultrasonic nebuliser was used to generate a H_20 NaCl aerosol, followed by a diffusion dryer, then a hose to supply either the sonde payload or a dilution unit, and finally an optical aerosol spectrometer. The diffusion dryer dehydrated the wet aerosol to give dry NaCl crystals. Aerosol output of this apparatus was observed to be relatively unstable upon being turned on, so the following graph (Figure 10) was obtained from an hour long test for calibration purposes.

To obtain a useful precipitator sample, the nebuliser was planned to be on for 15 minutes, but it was found that the ioniser current dropped to zero after only seven minutes. This resulted in a collected aerosol weight only slightly greater than the accuracy of our balance.

The ionisation current is plotted in figure 11. It seems reasonable to assume that this effect is due to the coating of salt deposited on the SEM target. As this is an insulator, and has become

[5] http://wiki.ukhas.org.uk/ideas:landing_spot_prediction

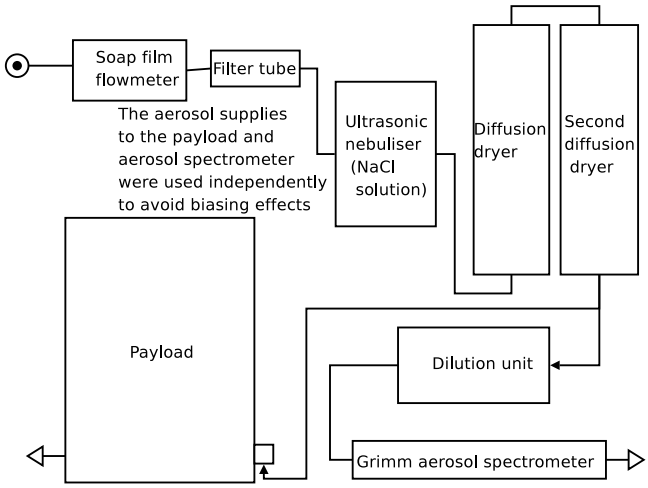

Figure 9: Schematic of the aerosol flow test experiment

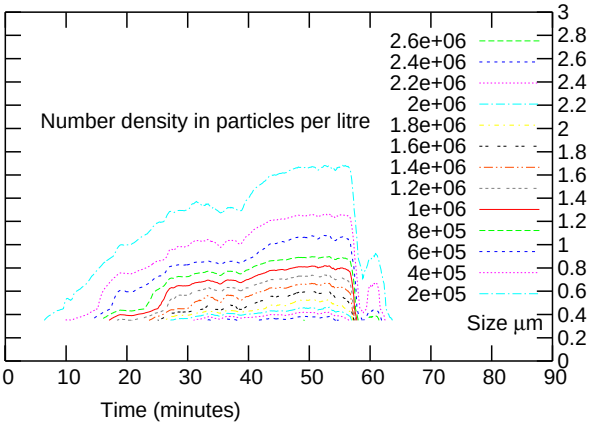

Figure 10: Contour plot of volumetric particle density from ultrasonic nebuliser against size bin, and run time

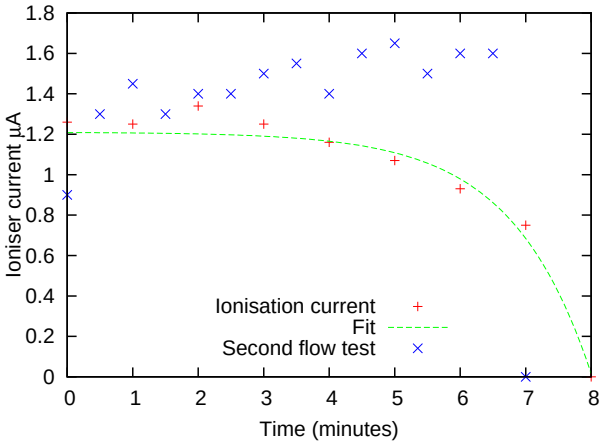

Figure 11: ioniser current plotted against time, with a function of the form $a + be^{cx}$ fitted to the data

Variable	Fit Value	Standard error
a	= 1.21	+/- 0.0468
b	= -0.00167	+/- 0.00165
c	= 0.821	+/- 0.121

Table 1: Fit of exponential to ionisation current

negatively charged from the corona discharge, once an insulating layer has built up a surface charge may accumulate. This reduces the electric field between the electrode rod and target until corona discharge no longer occurs, and the ionisation current drops to zero.

A fit of the form $a + be^{cx}$ was attempted for the first test data. In figure 11 the first, third and forth datapoints are not used in the fit, as the small increase in current at 2 minutes was believed to be due to increasing humidity as the nebuliser is turned on, not the target plane coating effect responsible for the current drop. In a second flow test however, the behaviour was somewhat different, with a higher current and a very sharp ionisation current cut off, so the effect clearly needs further investigation before any conclusions can be reached. One possible explanation is differing humidity of the aerosol stream, the silica gel in the diffusion dryers could have started to become saturated by the time of the last test.

Figure 12 shows the third SEM target, which was placed furthest upstream, after the first flow

Figure 12: The third SEM target after the test, showing a thick coating of salt

Figure 13: The second and first targets, the second target showing a slight dusting of salt

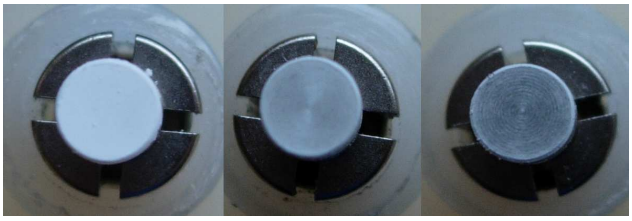

Figure 14: The SEM targets after the second flow test, third is lefter-most, first righter-most. The second showing a lighter coating of salt than the third, and the first only a slight dusting

test. It can been seen that the contamination of the second target (next downstream) was minimal (see figure 13) there was little visible deposition on the first target - furthest downstream.

In table 2 it can be seen that the collection ratios are at least $\frac{\Delta M_3}{\Delta M_2} < \frac{1}{3}$ and possibly $< \frac{1}{6}$ from the fact that the mass of the seconds target was $\pm$ one least significant digit both before and after the experiment. Unfortunately the limitations of the balance prevent further investigation.

Target	Start mass (mg)	Final mass	Difference
1	= 250.0	250.0	0.0
2	= 247.(0/1)	247.(0/1)	0.(0/1)
3	= 247.5	247.8	0.3
Filter	= 36240.2	36249.2	9.0

Table 2: Measured mass of the SEM targets and Filter Tube before and after the first flow test

Target	Start mass (mg)	Final mass	Difference
1	= 249.(8/9)	250.0	0.0
2	= 246.(8/9)	247.9	0.(0/1)
3	= 247.4	247.8	0.4
Filter	= 36248.4	36248.0	-0.4

Table 3: Measured mass of the SEM targets and Filter Tube before and after the second flow test

Interestingly the overall efficiency is low, considerably lower than Cheng et al [6] judging from the filter mass increase. However, some of this was shown to be due to moisture absorption by the second test results, where filter mass decreased. Secondly, although the nebuliser was turned off ten minutes into the experiment, the characterisation test shows that aerosol would have continued to enter the precipitator for some time after. Using the characterisation test results it would be possible to estimate how much aerosol passed through the instrument after the ionisation current dropped to zero. However the characterisation test had a longer run-time before the nebuliser was turned off, so has limited usefulness.

A second flow test was carried out to investigate efficiency further. The nebuliser and pump were turned off as soon as the ionisation current had dropped to zero, to avoid further aerosol entering the instrument. Interestingly, the filter mass was found to decrease (table 3). It was suspected that this was due to dehydration from the low humidity aerosol laden airflow - the filter had been left with both ends exposed to the laboratory air beforehand.

Leaving the filter tube in the laboratory to reach equilibrium humidity resulted in the mass increasing confirming the hypothesis (table 4). It would appear that the filter tube absorbed 0.0006 grams of salt, however we do not know how much aerosol is removed from the airstream by impaction with parts of the instrument- there was observed salt deposition on parts of the tubing. The filter mass measurement can thus only be used to put an upper limit on the total collection efficiency of $\frac{0.0004}{0.0004+0.0006} = 40\% \pm 7.2\%$.

An improved method for evaluating deposited aerosol quantities might be to dissolve in dis-

Time after experiment	Mass
15	36248.7
25	36248.9
54	36248.9
93	36249.0

Table 4: Filter mass in grams versus time in minutes after the filter was removed and allowed to reach humidity equilibrium with the lab air

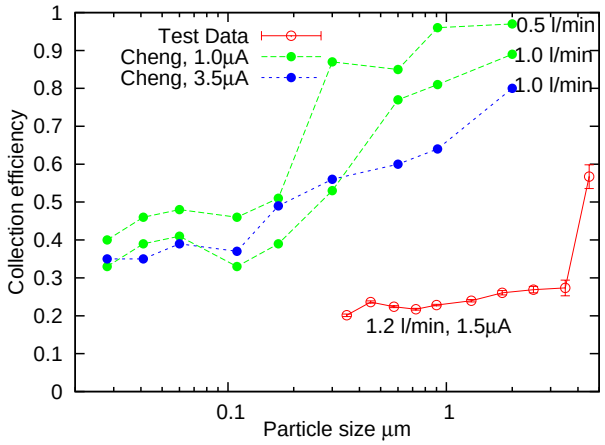

Figure 15: The collection efficiency as a function of particle size, error bars are one standard error. The results from Cheng et al [6] are also shown.

tilled water, then measure the conductivity to infer the NaCl content. Unfortunately all conductivity meters researched had insufficient accuracy to detect NaCl in the sub milligramme range. Yet another technique would be to use a titration technique to find the mass of salt.

The aerosol spectrometer however offers a more powerful technique: the spectrometer was placed on the electrostatic precipitator exhaust (with the pump and filters bypassed)[6], and the aerosol spectrum analysed with the high voltage on or off. A dilution unit being employed to reduce the particle number density to levels usable by the spectrometer. The results of this experiment are shown in figure 15

The fluctuation of the nebuliser output was a significant problem during the test. No attempt

[6]the aerosol spectrometer contains its own pump and volumetric flow control loop, so the payloads own pump had to be disconnected whilst the spectrometer was in use downstream of the precipitator

Variable	Final Value	Standard Error
a	= 282.896	+/- 12.64
b	= -0.0490468	+/- 0.00573
c	= 718.466	+/- 14.57

Table 5: Computed fit for figure 16

was made to accommodate this effect, and the errors were treated as random in the error bar calculation. From the aerosol spectrometer data it can be seem that although the number densities are far from constant with the ioniser on and off, the variation is mostly due to trends in the nebuliser output (see the appendix). A detrending technique such as a Fourier transform based filter or a linear trend applied over the duration of that the high voltage was applied (with a window either side) might help to improve this, as would running the experiment for longer before taking data (the experiment was conducted around 35 minutes after the nebuliser was turned on - from figure 10 it can be seen that waiting for over 50 minutes would have given more reliable data).

The control loop on the AVR driven daughterboard was evaluated during the (much longer duration) first flow test. As expected the volumetric flow rate was found to be linear with differential pressure across the filter, as predicted by Darcy's law, describing volumetric flow rate Q through a material of permeability κ.

$$Q = \frac{-\kappa A}{\mu} \frac{(P_b - P_a)}{L} \tag{6}$$

In the case of a filter, L is the membrane thickness, and $P_b - P_a$ the pressure drop across the filter. μ is the dynamic viscosity of the airflow, itself a function of temperature, as described in equation 5.

However, during the experiment, a long term drift in flow rate was observed. In figure 16 the flow rate is shown together with an exponential fit.

Setting different control loop set-points for the μC, and fitting with a straight line of the form $y = ax + b$, figure 17 was obtained.

Tables 6 and 7 give the linear fit parameter. It is interesting to note that the gain of the system,

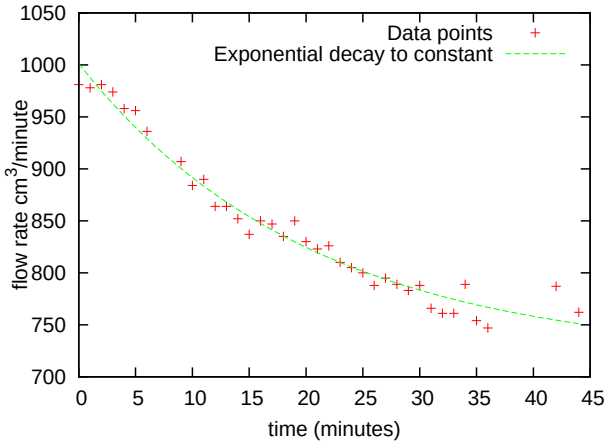

Figure 16: Test data over a 45 minute period, with an fit of the form $a \times e^{bt}$ where t is time in minutes

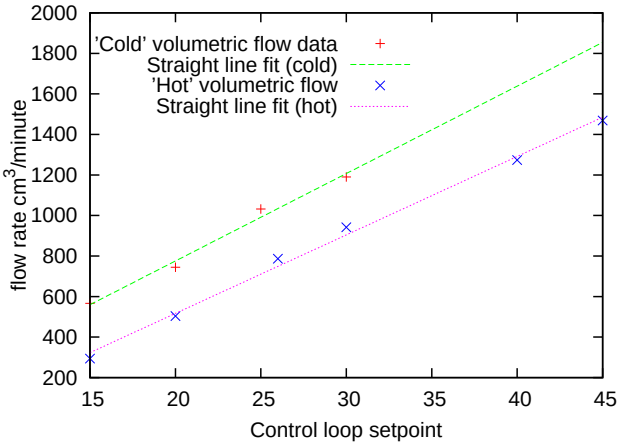

Figure 17: Data and Linnea fits for the control loop response straight after turn on, and after 45 minutes of operation

Variable	Fit Value	Standard error
a	= 43.14	+/- 3.437
b	= -87.3	+/- 79.69

Table 6: Linear fit to control system response at start of experiment

Variable	Fit Value	Standard error
a	= 38.7302	+/- 1.29
b	= -257.834	+/- 40.19

Table 7: Linear to control system response after 45 minutes

or a in the tables, changes by only slightly more than one standard error ($\sqrt{3.44^2 + 1.29^2} = 3.67$ as opposed to $43.14 - 38.73 = 4.41$, so it would appear that the exponentially falling response is due to the null of the pressure sensor, or b in our linear fit.

The change in the system null is $87.3 - 257.834 \pm \sqrt{40.19^2 + 79.69^2} = -170.53 \pm 89.251$. The predicted decay is given by $282.896(e^{-45 \times 0.0490468} - 1) = -251.77$ so this is within standard errors. Hence in summary it appears that the pressure sensor null is responsible for the drift in volumetric flow rate. A simple change to the AVR firmware, to turn off the pump and measure the differential pressure sensor null-point every 15 minutes or thereabouts was made to resolve the issue.

2.6.2 Software validation

As the main flight control software was written in python to run on a Linux system, it was a trivial matter to run on a ubuntu installation. In place of the pyserial module, files were used to simulate input and output from the embedded board. The most important function of the flight software is of course to enable a recovery of the payload after the flight, so GPS input needs to be replicated, and output to the radio and phone logged for analysis. The standard protocol for GPS chipsets is NMEA, a datapacket over serial protocol, where each packet has a header, data fields of comma seperated variables, and finally parity data to identify errors.

The university of Wyoming have produced an

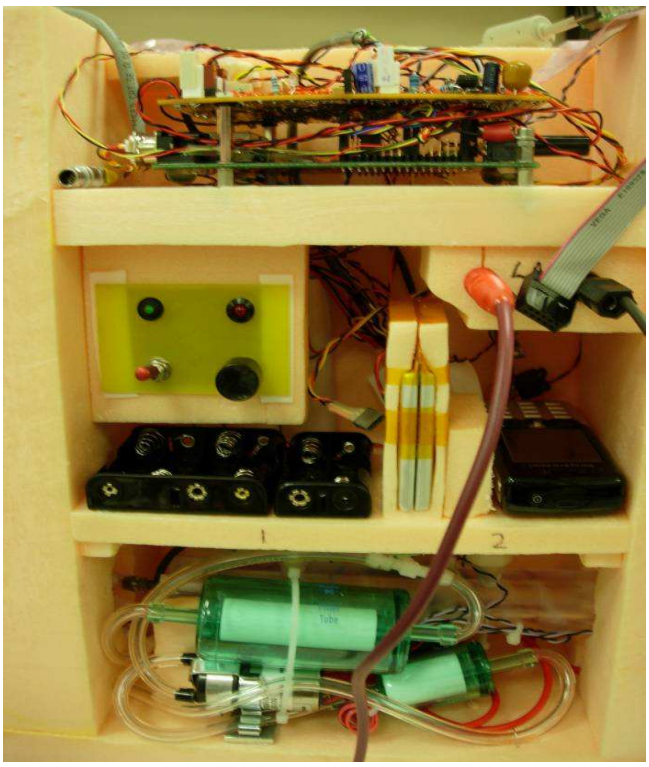

Figure 18: The assembled payload with the enclosure lid removed

online application for simulating balloon flights [7], which produces an output in Kml, and Xml format. A simple C program posted on the UKHAS wiki[8] was used to convert simulated flights into NMEA format. The flight code was thus tested under realistic flight conditions, allowing the landing spot prediction and polygon flight boundary, or "geofence" to be debugged, which would otherwise not have been possible. The flow tests also provided ample opportunity to debug the hardware interface code and avr.

3 conclusions

The sonde payload serves as a useful tool for atmospheric aerosol analysis, and is planned to be flown shortly by the Department.

The instrument allows three samples to be obtained at different vertical altitude ranges, but there is much room for improvement. Deposited particle density on the deposition surface is low, there is cross contamination between samples, and the overall number of sample targets could be increased to give greater vertical resolution.

[7] This can be found at http://weather.uwyo.edu/polar/balloon_traj.html

[8] Posted at http://wiki.ukhas.org.uk/code:emulator

References

[1] D.F. Blake and K. Kato, 1995: Latitudinal distribution of black carbon soot. Journal of geophysical research, Vol 100, No. D4, 7195-7202

[2] William C. Hinds, 1999, Aerosol technology, properties, behaviour, and measurement of airborne particles. Wiley.

[3] R.F. Pusechel and Coauthors, 1992: Black carbon (soot) aerosol in the lower stratosphere and upper troposphere. Geophysical Research lett., Vol 19, No. 16, 1659-1662

[4] Brenninkmeijer, C. A. M., and Coauthors, 1999: CARIBIC- Civil aircraft for global measurement of trace gases and aerosols in the tropopause region. J. Atmos. Oceanic Technol., 16, 1373-1383

[5] Snetsinger and Coauthors, 1987: Effects of the March-April 1982 El Chichon eruption on stratospheric aerosols, late 1982 to early 1984. Journal of Geophysical research, Vol 92, No. 14, 761-771

[6] Yung-sung Cheng et al, 1981: Collection efficiencies of a point-to-plane electrostatic precipitator. American industrial hygiene Ass. Journal, 42, 605-610.

[7] Alexander Laskin and James P. Cowin, 2001: On deposition efficiencies of a point-to-plane electrostatic precipitator. Journal of aerosol science, 33, 405-409

[8] Morrow, P.E., & Mercer, T. T. 1964: A point-to-plane electrostatic precipitator for particle size sampling, American industrial hygiene Ass. Journal, 25, 8-14

[9] UK Air Passenger Demand and CO2 Forecasts, Department for transport 2007.

[10] http://www.mil.ufl.edu/~chrisarnold /components/microcontrollerBoard/AVR/avrlib

[11] The UK high altitude society is a not for profit umberalla organisation to facilitate co-operation between UK high altitude balloon groups- http://www.ukhas.org.uk

[12] Cambridge University Spaceflight is a student organisation focused on high altitude and space flight- www.srcf.ucam.org/~cuspaceflight

[13] http://data.energizer.com/PDFs/l91.pdf